applied sciences

MDPI

Article

Process Technology for Development and Performance Improvement of Medical Radiation Shield Made of Eco-Friendly Oyster Shell Powder

Seon-Chil Kim

Department of Biomedical Engineering, School of Medicine, Keimyung University, 1095 Dalgubeol-daero, Daegu 42601, Korea; chil@kmu.ac.kr; Tel.: +82-10-4803-7773

Abstract: As radiation-based techniques become increasingly important tools for medical diagnostics, medical professionals face increasing risk from the long-term effects of scattered radiation exposure. Although existing radiation-shielding products used in medicine are traditionally lead-based, recently, the development of more eco-friendly materials such as tungsten, bismuth, and barium sulfate has drawn attention. However, lead continues to be superior to the proposed alternative materials in terms of shielding efficiency and cost effectiveness. This study explores the feasibility of radiation shielding materials based on the shells of bivalve mollusks such as oysters that are discarded from aquaculture, thereby preventing them from going into landfills. In addition, a firing process for enhancing the shielding efficiency of the original material is proposed. Experiments show that shielding sheets comprising 0.3 mm thick layers of oyster shell achieve a shielding efficiency of 37.32% for the low-energy X-rays typically encountered in medical institutions. In addition, the shielding efficiency was improved by increasing the density of the powdered oyster shell via plastic working at 1200 °C. This raises the possibility of developing multi-material radiation shields and highlights a new potential avenue for recycling aquaculture waste.

Keywords: eco-friendly material; radiation shielding; radiation shielding sheet; oyster shell

check for updates

Citation: Kim, S.-C. Process Technology for Development and Performance Improvement of Medical Radiation Shield Made of Eco-Friendly Oyster Shell Powder. *Appl. Sci.* **2022**, *12*, 968. https://doi.org/10.3390/app12030968

Academic Editor: Maria Filomena Botelho

Received: 15 December 2021
Accepted: 12 January 2022
Published: 18 January 2022

Publisher's Note: MDPI stays neutral with regard to jurisdictional claims in published maps and institutional affiliations.

Copyright: © 2022 by the author. Licensee MDPI, Basel, Switzerland. This article is an open access article distributed under the terms and conditions of the Creative Commons Attribution (CC BY) license (https://creativecommons.org/licenses/by/4.0/).

1. Introduction

Scattered radiation poses the risk of long-term exposure among medical professionals working in hospital radiography facilities [1–3]. To mitigate this risk, when operating radiation-emitting equipment, medical personnel wear protective aprons made of shielding sheets comprising a mixture of lead and rubber among other materials [4–7]. An apron with a lead equivalent of 0.25 mmPb weighs 3.25 kg, and an apron with a lead equivalent of 0.5 mmPb weighs approximately 4.95 kg [8,9]. These weights, however, limit their activity. To address this problem, the development of new radiation-shielding materials, with lighter, more eco-friendly materials including tungsten, bismuth, barium, boron, and tin among the proposed alternatives is extensively studied [10–14]. These lead substitutes are not susceptible to the risks associated with heavy metals; however, to be used for radiation-shielding sheets, they must be compatible with polymeric materials [15,16]. In addition, the cost effectiveness of new shielding materials is an important factor with respect to their commercial prospects. Therefore, researchers face the challenge of providing shielding materials that are economical and that meet weight and human safety requirements.

This study explores the viability of developing radiation-shielding materials by processing oyster shells that would otherwise be discarded as general waste. Various shellfish, such as oysters, clams, and mussels, which live in coastal waters, can be collected for processing. These shellfish are characterized by a large volume of shell compared to the flesh it houses. Further, the large number of shells discarded from aquaculture are a major source of waste that contributes to environmental pollution along coastlines and in landfills [17,18].

Currently, the shell recycling industry is very limited, and in certain cases, shells are recycled as soil fertilizer. However, this industry does not have significant economic value [19]. The main component of these shells is calcium, with an atomic number of 20 and a density of 1.55 g/cm^3 [20]. It also reacts easily with oxygen and water, and exists in the form of a calcium carbonate compound in nature. Compared to lead with an atomic number of 82 and a density of 11.34 g/cm^3, calcium exhibits inferior radiation shielding [21].

Oyster shell is easy to process because it contains a large amount of salt and has a porous structure. In addition, it shows excellent affinity for mixing with other materials, and is therefore being studied as an aggregate for construction materials. Additionally, oyster shell has been mixed with concrete during research on gamma ray shielding [22,23].

As oyster shells exhibit excellent compatibility with materials such as concrete [24], this study predicted that the particle structure would be dense, and its density could be increased even after mixing with polymer materials. Therefore, this study attempted to improve shielding efficiency by manufacturing a radiation shielding sheet using oyster shells. To this end, the characteristics of powdered oyster shell were analyzed by conducting plastic working at different temperatures, and evaluating the particle distribution according to the cross-sectional structure of a polymer-based shielding sheet. Furthermore, the effect of plastic working technology on the shielding efficiency of oyster shell was analyzed, and the degree of dispersion within the polymer material was evaluated. In addition to powdered oyster shell, shielding sheets based on barium sulfate, tungsten, and bismuth oxide were manufactured using the same process, and their shielding efficiencies compared. Therefore, the relationship between plastic working and shielding efficiency was analyzed for radiation shields that are based on powdered oyster shell, and this relationship was evaluated against existing shielding sheets that are based on safer lead alternatives.

2. Materials and Methods

Oysters were collected from the coasts of Nosan-ri, Gwangdo-myeon, and Tongyeong (South Korea). First, the flesh was separated from the shells, and then the shells (Figure 1) were washed with distilled water and dried for 12 h at 80 °C using a hot air dryer. Next, the dried shells were pulverized, and the particles were sieved using a micromesh to ensure a uniform particle size. To perform plastic working, the refined oyster shell powder was subjected to heat treatment ranging from 600 °C to 1200 °C using muffle furnaces (Nabertherm, Co., Lilienthal, Germay; model: L5/11). Throughout this process, changes were observed in the morphology of the particles, and shielding sheets were manufactured by mixing the powdered oyster shell with a polymer.



Figure 1. Oyster shells collected from the coasts of Nosan-ri, Gwangdo-myeon, and Tongyeong-si (South Korea).

Figure 2 shows photographs of refined oyster shell powder prior to plastic working and after plastic working at 600 °C and 1200 °C. To produce the radiation shielding sheet samples, high-density polyethylene (HDPE) was selected as the polymer material and mixed with the powdered oyster shell and the base material. Owing to its excellent

strength, HDPE is mainly used as a disposable plastic product [25]. The HDPE used in this study had a molecular weight of ≥4,000,000 g/mol and a density of 0.91 g/cm^3.



Figure 2. Oyster shell powder heat-treated using plastic working: (**a**) freshly pulverized powder without heat treatment; (**b**) powder after plastic working at 600 °C; and (**c**) powder after plastic working at 1200 °C.

To make the final composite materials, N-dimethylformamide (DMF, 99.5%) was used to make a casting solution. Next, DMF (~ 10 wt%) and powdered oyster shell (70 wt%) were placed in a stirrer and stirred at 5000 rpm to disperse the particles. Diisononyl phthalate (DINP, 0.85–0.95 wt%) was used as a plasticizer to remove the voids inside the shielding sheet. To ensure the uniformity of the shielding efficiency of the final casting solution, contaminants were removed through filtering and defoaming, with the sheet finished using a compression molding calendar process. The final shielding sheets measured 300 mm × 300 mm × 0.3 mm. The appearances of the manufactured shielding sheets are shown in Figure 3. This process was repeated to fabricate shielding sheets using barium sulfate, bismuth oxide, and tungsten, and their respective shielding efficiencies were compared. Each of the manufactured shielding sheets had the same shielding material capacity and the same dimensions.

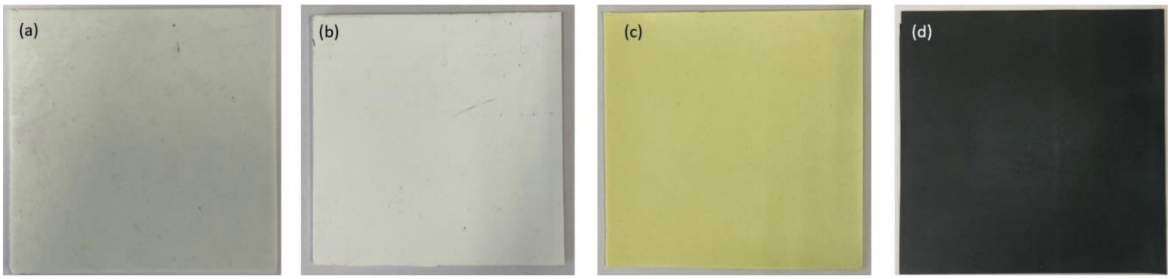

Figure 3. Comparing appearances of shielding sheets manufactured using the same process: (**a**) powdered oyster shell (1200 °C), (**b**) barium sulfate, (**c**) bismuth oxide, and (**d**) tungsten.

The particle dispersibility of the shielding materials was observed using field-emission scanning electron microscopy (FE-SEM; S-4800, Hitachi) after thin-film sectioning using a microtome (RM2235, Leica).

Radiation transmission characteristics were used to evaluate the shielding efficiency of the sheets. When radiation passes through a medium, that is, a material, the change in the incident energy due to the nuclei and electrons leads to attenuation. Therefore, to increase the attenuation effect of the incident energy, it is necessary to provide the maximum possible time for the interaction to occur within the material through which the radiation passes. As the thickness of the shielding sheet increases, its range of interaction also increases, and consequently, thickness can serve to increase the interaction time. The degree of reduction with respect to the radiation energy per unit distance traveled in the shielding material is represented by the linear attenuation coefficient [26]:

$$\begin{aligned} I &= I_0 e^{-(\mu_1 x_1 + \mu_2 x_2)} \\ \mu_1 &= \frac{\left[In\left(\frac{I_0}{I}\right) - \mu_2 x_2\right]}{x_1}, \end{aligned} \tag{1}$$

where I and I_0 are the intensities of transmitted and incident energies, respectively; μ_1 and μ_2 are the linear attenuation coefficients of the shielding material and air, respectively; and x_1 and x_2 are the thickness of the shielding sheet and the distance from the radiation source to the shielding sheet, respectively.

The intensity of the radiation incident energy is attenuated by the linear attenuation coefficient of the material as it passes through the thickness of the shielding sheet made of the oyster shell. Therefore, if the thickness of the shielding sheet is fixed, the linear attenuation coefficient, which is a function of the radiation energy, can be calculated using Equation (1). In a shielding sheet with a constant thickness, medical radiation energy is inversely proportional to the shielding efficiency, and the higher the intensity of the incident energy, the lower the shielding efficiency [27]. As a result, the greater the interaction due to the dispersion of oyster shell powder particles in the shielding sheet, the greater the shielding efficiency owing to the attenuation of the radiation energy. In this study, plastic working was used to reduce the inter-particle spacing and increase the number of interactions with incident radiation. Therefore, the degree of dispersion of the oyster shell powder particles in the shielding sheet according to the process technology results and the affinity with the base material were observed under a microscope.

The shielding efficiency of the various shielding sheet samples was tested using the setup shown in Figure 4. The measurement method was applied in compliance with the lead equivalent test method (KS A 4025: 2017) [28]. The radiation, which is the complex energy used in the experiment, was expressed as a single energy, that is, the effective energy, log_e was performed on both sides of the attenuation coefficient law ($I = I_0 e^{-\mu x}$), where x is the attenuation thickness, and the slope of the graph of $y = -ax$ is used to measure the half-value layer. In addition, after obtaining the linear absorption coefficient, μ, from this slope, the half-value layer was calculated as $0.693/\mu$ [29]. For the effective energy calculation, Hubbell's mass absorption coefficient table was used to calculate the effective energy corresponding to the calculated half-value layer [30]. The shielding rate of the sheets was calculated as $(1 - W/W_0) \times 100$ [31], where W and W_0 are the doses measured with and without a shielding sheet between the X-ray tube and the dosimeter, respectively. A total of 10 measurements were performed using an X-ray generator (Toshiba E7239, 150 kV–500 mA, 1999, Tokyo, Japan), and the calculated average value was applied. The dose detector was DosiMax plus I (2019 IBA Dosimetry Corp., Schwarzenbruck, Germany), which was used after testing and calibration.

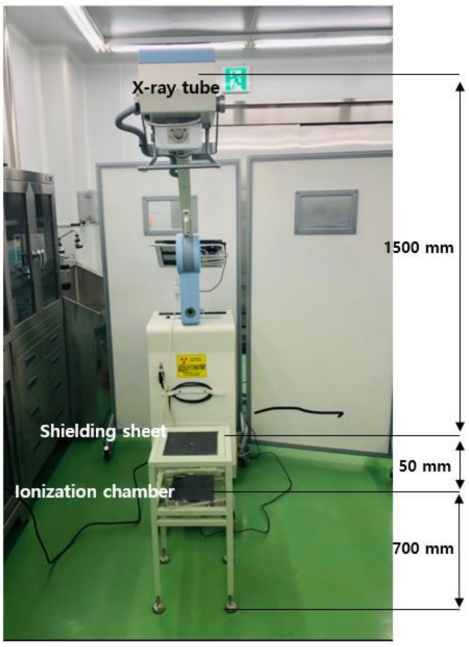

Figure 4. Experimental setup for evaluating the shielding efficiency of the sheet materials.

3. Results

Figure 5 shows the morphological changes in the oyster shell particle in response to being heated for plastic working. Compared with the untreated particles in Figure 5a, plastic working reduces the distance between the particles in Figure 5b,c, which correspond to temperatures of 600 °C and 1200 °C, respectively. The inter-particle spacing affects the density of the shielding material, thereby directly affecting its shielding efficiency [32].

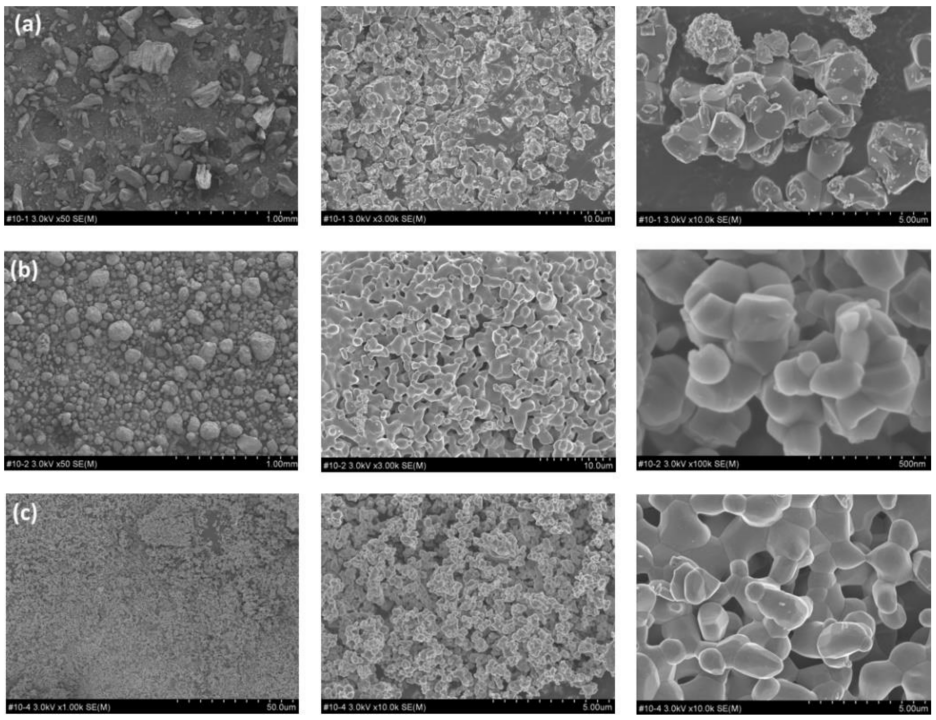

Figure 5. SEM images providing a comparative analysis of oyster shell particle morphology and spacing in response to plastic working: (**a**) untreated oyster shell particles, (**b**) particles after plastic working at 600 °C, and (**c**) particles after plastic working at 1200 °C.

Table 1 lists the thicknesses, weights, and densities of the three oyster shell sample variations. Through plastic working, the particle size and number of voids are reduced, thus increasing the density of the sheet.

Table 1. Physical properties of the fabricated oyster shell-based shielding sheets.

	Thickness (mm)	Weight (g)	Density (g/cm^3)
Oyster shell sheet without heat treatment	0.32	23.39	8.12
Oyster shell sheet with plastic working at 600 °C	0.31	28.12	10.07
Oyster shell sheet with plastic working at 1200 °C	0.32	31.25	10.85

In addition, the particle distribution within the oyster shell-based samples was analyzed by performing SEM imaging of sheet cross-sections (Figure 6). Oyster shell powder processed at high temperature mixed excellently with polymer materials, and the particle distribution was extensive when compared at the same magnification. In addition, mixing the processed oyster shell powder with HDPE changed the distribution state of the powder particles, as shown in Figure 6, but the visual properties remained intact.

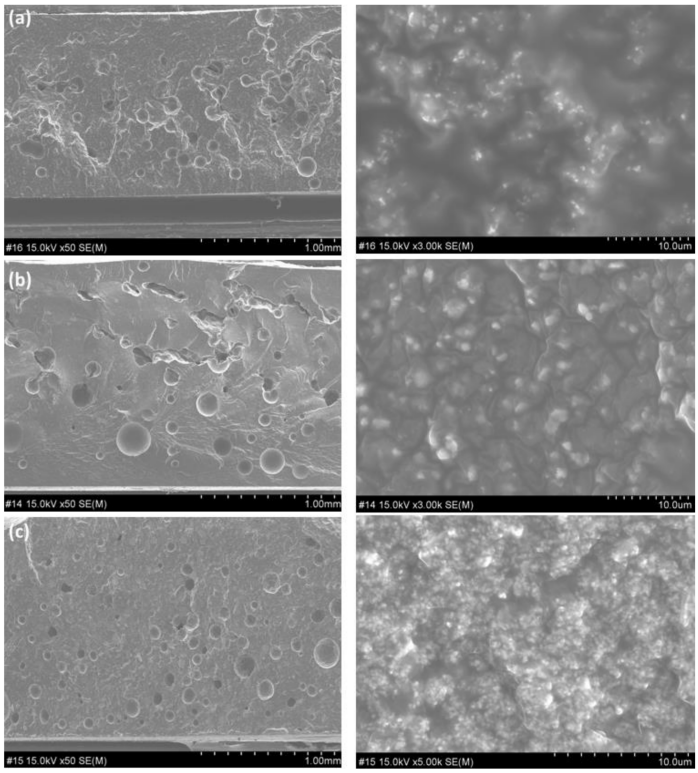

Figure 6. SEM images of sheet cross-sections providing a comparative analysis of the oyster shell particle morphology in the plastic working state: (**a**) untreated oyster shell particles, (**b**) particles after plastic working at 600 °C, and (**c**) particles after plastic working at 1200 °C.

Tables 2 and 3 present the experimental results for the shielding efficiency of the oyster shell sheet presented in this study. First, the shielding rate of the oyster shell sheet based on the plastic working temperature was compared to that of the shielding sheet manufactured through the same process as that of the eco-friendly shielding material, and evaluated.

Table 2 shows the shielding efficiency of the oyster shell sheet based on the temperature during plastic working, and the shielding rate of the shielding sheet processed at 1200 °C was the highest. The experimental data reveal that the oyster shell powder without plastic working provides a low shielding efficiency of approximately 18% in the low-energy X-ray region; however, this increases to approximately 37% for the sheet fabricated using plastic working at 1200 °C. Table 3 shows the results of comparing the shielding sheets made of barium sulfate, bismuth oxide, and tungsten, which are the most used main materials for eco-friendly shielding sheets. As a result, the oyster shell sheet processed at 1200 °C showed an average shielding efficiency that was 7.2% lower than that of the barium sulfate shielding sheet, which had the lowest shielding efficiency. In addition, a lead sheet of an equivalent of 0.3 mm, with the same thickness, is almost shielded, and the oyster shell sheet can be predicted to have a shielding efficiency that is approximately 40% of the lead efficiency.

Table 2. Comparison between the shielding efficiencies of oyster shell-based shielding sheets fabricated with and without plastic working.

X-ray Tube Voltage (kVp)	Effective X-ray Energy (keV)	Mean Exposure (μR)				Shielding Rate (%)		
		Nothing	0 °C	600 °C	1200 °C	0 °C	600 °C	1200 °C
40	24.6	106.90	87.72	84.47	67.01	17.94	20.98	37.32
60	28.7	381.63	334.07	320.83	278.97	12.46	15.93	26.90
80	32.5	799.70	738.57	702.13	630.80	7.64	12.20	21.12
100	48.5	1318.33	1199.00	1180.67	1079.67	9.05	10.44	18.10
120	54.9	1648.33	1510.33	1484.67	1372.67	8.37	9.93	16.72

Table 3. Comparison between the shielding efficiencies of eco-friendly shielding sheets.

X-ray Tube Voltage (kVp)	Effective X-ray Energy (keV)	Mean Exposure (μR)						Shielding Rate (%)				
		Nothing	Pb	Oyster Shell (1200 °C)	Barium Sulfate	Bismuth Oxide	Tungsten	Pb	Oyster Shell	Barium Sulfate	Bismuth Oxide	Tungsten
40	24.6	106.90	0	67.01	61.04	41.69	19.23	100	37.32	42.90	61.00	82.01
60	28.7	381.63	6.47	278.97	236.51	160.15	114.36	98.30	26.90	38.03	58.04	70.03
80	32.5	799.70	48.87	630.80	550.80	463.81	351.76	93.89	21.12	31.12	42.00	56.01
100	48.5	1318.33	144.83	1078.67	1001.93	870.03	672.26	89.01	18.10	24.00	34.01	49.01
120	54.9	1648.33	207.43	1372.67	1318.66	1120.76	906.05	87.42	16.72	20.00	32.01	45.03

4. Discussion

Radiation-shielding equipment in medical institutions relies mainly on lead, whose toxicity has created urgency for an alternative [33–36]. This study investigated the potential of powdered oyster shell as a new eco-friendly shielding material. The seafood industry generates a vast amount of waste in the form of discarded shells such as oyster shells, much of which goes to landfills. As such, the recycling of oyster shells is an important issue because of the environmental pollution caused by odors and leachate from their waste, and the damage they cause to the natural landscape [37–39]. Therefore, the radiation-shielding efficiency was evaluated to broaden the scope of shellfish recycling. Table 4 summarizes the composition of several types of shellfish [40]; furthermore, calcium carbonate accounts for the vast majority in each case. Oyster shells are the most abundant of the shells discarded by aquaculture and are easily accessible [41]. Moreover, the radiation shielding efficiency of limestone has been studied [42], and limestone has been observed to comprise calcium carbonate as its main component.

Table 4. Chemical compositions of different shellfish [19].

Type of Shellfish	Elemental Composition (%)						
	CaO	Na_2O	CI/MnO	SiO_2	SO_3	AI_2O_3	Fe_2O_3
Clams	94.97	1.01	-	1.83	0.52	0.45	0.58
Cockles	95.95	-	-	1.68	0.65	0.58	0.59
Manila clams	92.79	1.13	0/0.13	3.09	0.59	0.98	0.63
Oysters	84.59	5.92	5.15/0	1.63	1.19	0.45	0.32

As the low density of calcium carbonate has a significant impact on its shielding effect, plastic working was investigated as a means of increasing its density and enhancing its radiation-attenuation capacity. This approach was reasonably successful, with plastic working reducing the inter-particle distance by decreasing the distance from the center of

the particles to their edges. Consequently, it is possible to increase the relative density by adding particles within the same space. This approach improved the shielding efficiency, with the shielding efficiency of the oyster shell material produced using plastic working at 1200 °C being more than double that of the sheet fabricated without plastic working. During plastic working, calcium carbonate changes to calcium oxide within a certain temperature range; therefore, the characteristics of the heat-treated oyster shell powder sheet reflect those of calcium oxide.

Therefore, as shown in the results of this experiment, the shielding efficiency of eco-friendly shielding materials other than tungsten is insufficient to be used alone. However, in the case of oyster shell powder, if other materials, such as tungsten, are mixed and used, it is considered that the low weight and cost effectiveness of the shield can be achieved. In addition, it should be noted that barium sulfate is considered adequate for shielding against the lower doses received from scattered rays, and the shielding efficiency of the heat-treated oyster shell powder was approximately 7.2% lower than that of barium sulfate, indicating its potential as a shielding material that can be mixed with other materials.

5. Conclusions

This study evaluated the shielding performance by manufacturing a radiation shielding sheet that can be used in medical institutions using oyster shell powder that is discarded as daily waste. The manufactured oyster shell shielding sheet showed an average of 32% shielding efficiency in the low energy range of less than 30 keV effective energy of medical radiation, and 18.6% in the high energy range of 30 keV or more. In addition, in the processing method of the oyster shell powder, a technology for improving the shielding efficiency by increasing the inter-particle density through plastic working at 1200 °C was presented.

This study tried to predict the shielding performance when used as a mixed material by discovering a new shielding material and evaluating its shielding performance. As a process technology, plastic working proved effective in increasing the shielding sheet density relative to that based on pure oyster shell powder, and could similarly benefit other materials.

A mixture that can be mixed with the shielding material is needed to satisfy the light weight requirement of radiation shields for medical institutions. Through this study, a process technology that can utilize oyster shell powder, which is discarded as waste, as an economical mixed material was presented. These results could be an important objective for future research on radiation shields used in medical institutions.

Funding: This work was supported by the National Research Foundation of Korea (NRF) grant funded by the Korea government (MEST) (NRF. 2020R1I1A3070451).

Institutional Review Board Statement: Not applicable.

Informed Consent Statement: Not applicable.

Data Availability Statement: Data is contained within the article.

Conflicts of Interest: The author declares no competing interests.

References

1. Mahadevappa, M. Radiation dose management for fluoroscopically guided interventional medical procedures. National Council on Radiation Protection and Measurements. *Int. J. Med. Physiol.* **2010**, *21*, 5789–5790. [CrossRef]
2. United Nations Scientific Committee on the Effects of Atomic Radiation. *Sources and Effects of Ionizing Radiation*; UNSCEAR 2008 REPORT 1; UNSCEAR: New York, NY, USA, 2010.
3. López, P.O.; Dauer, L.T.; Loose, R.; Martin, C.J.; Miller, D.L.; Vañó, E.; Doruff, M.; Padovani, R.; Massera, C.; Yoder, C. ICRP Publication 139, 2017 Occupational Radiological Protection in Interventional Procedures. *Ann. ICRP* **2017**, *47*, 1–118. [CrossRef]
4. Dominique, A.; Marc, P.; Fabien, B.; Redha, T.; Guillaume, P. Wearing lead aprons in surgical operating rooms: Ergonomic injuries evidenced by IR Thermography. *J. Surg. Res.* **2017**, *209*, 227–233. [CrossRef]
5. Zuguchi, M.; Chida, K.; Taura, M.; Inaba, Y.; Ebata, A.; Yamada, S. Usefulness of non-lead aprons in radiation protection for physicians performing interventional procedures. *Radiat. Prot. Dosim.* **2008**, *131*, 531–534. [CrossRef]

6. Marichal, D.A.; Anwar, T.; Kirsch, D.; Clements, J.; Carlson, L.; Savage, C.; Rees, C.R. Comparison of a Suspended Radiation Protection System versus Standard Lead Apron for Radiation Exposure of a Simulated interventionalist. *J. Vasc. Interv. Radiol.* **2011**, *22*, 437–442. [CrossRef]
7. Livingstone, R.S.; Varghese, A.; Keshava, S.N. A study on the use of radiation-protective apron among interventionists in radiology. *J. Clin. Imaging Sci.* **2008**, *8*, 1–4. [CrossRef] [PubMed]
8. Lu, H.; Boyd, C.; Dawson, J. Lightweight lead aprons: The emperor's new clothes in the angiography suite? *Eur. J. Endovasc. Surg.* **2019**, *57*, 730–739. [CrossRef] [PubMed]
9. Kumar, S.; Moro, L.N.; Narayan, Y. Perceived physical stress at work and musculoskeletal discomfort in X-ray technologists. *Ergonomics* **2004**, *47*, 189–201. [CrossRef]
10. Cai, Y.; Hu, H.; Lu, S.; Jia, Q. Optimization of radiation shielding material aiming at compactness, lightweight, and low activation for a vehicle-mounted accelerator-driven DT neutron source. *Appl. Radiat. Isot.* **2018**, *135*, 147–154. [CrossRef] [PubMed]
11. Soylu, H.M.; Lambrecht, F.Y.; Ersöz, O.A. Gamma radiation shielding efficiency of a new lead-free composite material. *J. Radioanal. Nucl. Chem.* **2015**, *305*, 529–534. [CrossRef]
12. Çetin, H.; Yurt, A.Y.; Yüksel, S.H. The Absorption properties of lead-free garments for use in radiation protection. *Radiat. Prot. Dosim.* **2017**, *173*, 345–350. [CrossRef] [PubMed]
13. AbuAlRoos, N.J.; Azman, M.N.; Amin, N.A.B.; Zainon, R. Tungsten-based material as promising new lead-free gamma radiation shielding material in nuclear medicine. *Phys. Med.* **2020**, *78*, 48–57. [CrossRef]
14. Adlienė, D.; Gilys, L.; Griškonis, E. Development and characterization of new tungsten and tantalum containing composites for radiation shielding in medicine. *Nucl. Instrum. Methods Phys. Res. Sect. B Beam Interact. Mater. At.* **2020**, *467*, 21–26. [CrossRef]
15. Kim, Y.K.; Park, S.G.; Seo, Y.S. Enhanced X-ray Shielding Ability of Polymer–Nonleaded Metal Composites by Multilayer Structuring. *Ind. Eng. Chem. Res.* **2015**, *54*, 5968–5973. [CrossRef]
16. Li, Q.; Wei, Q.; Zheng, W.; Zheng, Y.; Okosi, N.; Wang, Z.; Su, M. Enhanced radiation shielding with conformal light-weight nanoparticle–polymer composite. *ACS Appl. Mater.* **2018**, *10*, 35510–35515. [CrossRef] [PubMed]
17. Kim, H.M.; Alengaram, U.J.; Jumaat, M.Z.; Lee, S.C.; Goh, W.I.; Yuen, C.W. Recycling of seashell waste in concrete: A review. *Constr. Build Mater.* **2018**, *20*, 751–764. [CrossRef]
18. Yao, Z.; Xia, M.; Li, H.; Chen, T.; Ye, Y.; Zheng, H. Bivalve shell: Not an abundant useless waste but a functional and versatile biomaterial. *Crit. Rev. Environ. Sci. Technol.* **2014**, *44*, 2502–2530. [CrossRef]
19. Chung, C.W. Possibility to recycle domestic waste shells-with emphasis on oyster shells. *Mag. Concr. Res.* **2016**, *11*, 11–16. [CrossRef]
20. Owuamanam, S.; Cree, D. Progress of bio-calcium carbonate waste Eggshell and seashell fillers in polymer Composites: A review. *Compos. Sci. Technol.* **2020**, *4*, 70. [CrossRef]
21. Elsheikh, N.A.A. Monte Carlo modelling of a neutron-induced gamma-ray sensor for landmine or explosive detection. *J. Radiat. Res. Appl. Sci.* **2018**, *11*, 403–407. [CrossRef]
22. Chiou, I.J.; Chen, C.H.; Li, Y.H. Using oyster-shell foamed bricks to neutralize the acidity of recycled rainwater. *Constr. Build Mater.* **2014**, *64*, 480–487. [CrossRef]
23. Seo, J.H.; Park, S.M.; Yang, B.J.; Jang, J.G. Calcined oyster shell powder as an expansive additive in cement mortar. *Materials* **2019**, *12*, 1322. [CrossRef]
24. Chen, D.; Zhang, P.; Pan, T.; Liao, Y.; Zhao, H. Evaluation of the eco-friendly crushed waste oyster shell mortars containing supplementary cementitious materials. *J. Clean. Prod.* **2019**, *237*, 1–33. [CrossRef]
25. Rahman, T.; Nurdiana, J. The effect of HDPE plastic fibres on concrete performance. *Resour. Recycl.* **2020**, *5*, 1–16. [CrossRef]
26. Kim, S.C. Development of air pressure mirroring particle dispersion method for producing high density tungsten medical radiation shielding film. *Sci. Rep.* **2021**, *11*, 1–10. [CrossRef]
27. Maghrabi, H.A.; Vijayan, A.; Mohaddes, F.; Deb, P.W.; Wang, L. Evaluation of X-ray radiation shielding performance of barium sulphate-coated fabrics. *Fibers Polym.* **2016**, *17*, 2047–2054. [CrossRef]
28. Korean Standards Association. *Testing Method of Lead Equivalent for X-Ray Protective Devices*; KSA 4025; Korean Standards Association: Seoul, Korea, 2017.
29. Kaur, T.; Sharma, J.; Singh, T. Experimental evaluation of gamma rays shielding parameters for Zn-Cd-Sn-Pb quaternary alloy. *Radiat. Phys. Chem.* **2019**, *156*, 193–198. [CrossRef]
30. Hubbell, J.H. Photon Mass Attenuation and Energy absorption Coefficients from 1 keV to 20 MeV. *Int. Appl. Radiat. Isot.* **1982**, *33*, 1269–1290. [CrossRef]
31. Pingale, P.L. Formulation, evaluation of fast dissolving tablet of anti-HIV drugs as fixed dose combination: Use of freeze-dried powder of Annona reticulata and comparison WITH synthetic superdisintegrants. *J. Pharm. Sci. Innov.* **2019**, *8*, 38–41. [CrossRef]
32. Xie, T.; Xu, K.; Yang, B.; He, Y. Effect of pore size and porosity distribution on radiation absorption and thermal performance of porous solar energy absorber. *Sci. China Technol. Sci.* **2019**, *62*, 2213–2225. [CrossRef]
33. AbuAlRoos, N.J.; Amin, N.A.B.; Zainon, R. Conventional and new lead-free radiation shielding materials for radiation protection in nuclear medicine: A review. *Radiat. Phys. Chem.* **2019**, *165*, 108439. [CrossRef]
34. Johansen, S.; Hauge, I.H.R.; Hogg, P.; England, A.; Lança, L.; Gunn, C.; Sanderud, A. Are Antimony-Bismuth Aprons as Efficient as Lead Rubber Aprons in Providing Shielding against Scattered Radiation? *J. Med. Imaging Radiat. Sci.* **2018**, *49*, 201–206. [CrossRef]

35. Mori, H.; Koshida, K.; Ishigamori, O.; Matsubara, K. Evaluation of the effectiveness of X-ray protective aprons in experimental and practical fields. *Radiol. Phys. Technol.* **2014**, *7*, 158–166. [CrossRef] [PubMed]
36. Yue, K.; Luo, W.; Dong, X.; Wang, C.; Wu, G.; Jiang, M.; Zha, Y. A new lead-free radiation shielding material for radiotherapy. *Radiat. Prot. Dosim.* **2009**, *133*, 256–260. [CrossRef] [PubMed]
37. Nam, G.; Lee, N.J.; Ahn, J.W. Sustainable management of oyster shell by-products and recent research techniques. *J. Energ. Eng.* **2018**, *27*, 1–11. [CrossRef]
38. Kwon, H.B.; Lee, C.W.; Jun, B.S.; Weon, S.Y.; Koopman, B. Recycling waste oyster shells for eutrophication control. *Resour. Conserv. Recycl.* **2004**, *41*, 75–82. [CrossRef]
39. Ramakrishna, C.; Thenepalli, T.; Han, C.; Ahn, J. Synthesis of aragonite-precipitated calcium carbonate from oyster shell waste via a carbonation process and its applications. *Korean J. Chem. Eng.* **2017**, *34*, 225–230. [CrossRef]
40. Lu, J.C.; Li, X.; Hao, Y.; Wang, Y.C. Scalable recycling of oyster shells into high purity calcite powders by the mechanochemical and hydrothermal treatments. *J. Clean. Prod.* **2017**, *172*, 1978–1985. [CrossRef]
41. Silva, T.H.; Mesquita-Guimarães, J.; Henriques, B.; Silva, F.S.; Fredel, M.C. The potential use of oyster shell waste in new value-added by-product. *Resources* **2019**, *8*, 13. [CrossRef]
42. Sharaf, J.M.; Saleh, H. Gamma-ray energy factor calculations and shielding effects of some Jordanian building structures. *Radiat. Phys. Chem.* **2015**, *110*, 87–95. [CrossRef]